Institute of Space and Aeronautical Science, University of Tokyo
Report No. 570, March 1979

An Analytical Investigation of the Transient Ablation of Teflon in Convective and Radiative Environments

By

Norio ARAI

Summary: On the basis of this investigation of the high temperature behavior of polytetrafluoroethylene (PTFE), the transient one-dimensional ablation of PTFE has been developed by taking into account the optical transmittance of both the amorphous zone and the crystalline zone of PTFE-layer. Results show that although the exposed surface receded at an apparently steady state, both the internal temperature and the thickness of the gel layer increase continuously due to the internal absorption of radiation.

NOMENCLATURE

A_p	effective collision frequency
C	fraction of mass of oxygen in a boundary layer
C_p	specific heat
E	activation energy
h_m	heat of transition
h_v	reaction heat per unit mass of oxygen
H_0	stagnation enthalpy of the gas
H_p	local depolymerization energy
ΔH_w	enthalpy difference over the boundary layer
I	radiation intensity
I_e	external incident radiation intensity
k	thermal conductivity
K	absorption coefficient
L_0	initial thickness of the ablating body
m	index on radiation bands that penetrate the body
$\dot{m}$	ablation rate
n	index on radiation bands absorbed at the exposed surface and index of refraction
q_0	convective heating rate without mass injection
q_r	incident radiative heating rate at the exposed surface

This report is a study which was conducted at NASA Ames Research Center, Moffett Field, CA, U.S.A. during 1977 to 1978 under the grant of National Research Council Associateship.

q_{rad} total incident radiative flux absorbed at the exposed surface
Q_p depolymerization energy per unit volume
Q_R total radiation flow in the ablating body
r reflectivity
R universal gas constant
s position of the surface
$\dot{s}$ ablation velocity, ds/dt
S scattering coefficient
t time
T temperature
x spacial coordinate
δ_{hs} thickness of the heat sink
ε surface emissivity
θ thickness of the gel layer
$\dot{\theta}$ growing rate of the gel layer, $d\theta/dt$
ρ density
ψ correction factor by mass injection
ξ transformed coordinate

Subscripts:

b conditions at the backface
B blackbody
e external incident radiative intensity
hs heat sink
i internal reflection coefficient and interface
m conditions at the phase change
R outward direction in the ablating body
s surface
T inward direction in the ablating body
ν the νth spectral band of radiation being absorbed and/or reflected at the exposed surface
1 conditions in the gel layer
2 conditions in the solid layer

1. Introduction

For high-speed entry of space vehicles into atmospheric environments, ablation cooling is a practical method for protecting surfaces from severe heat fluxes and for limiting material temperatures. In particular, the entry heating environment for a probe entering the large planets, such as Jupiter and Saturn, is a severe one in which radiative heat loads are associated with convective heat loads. The ablating heat shields used in the past to protect probes from convective heating may not be adequate for these additional heat loads. For such entries, ablators will have to be

chosen to withstand both the radiative and the convective heating.

One method, which is now being developed to withstand the radiative and convective heat load, uses reflecting ablation heat shields [*1–3*]. A dielectric material is used to reflect the radiative heat load diffusely rather than a metallic material to specularly reflect it. A heat shield using a dielectric material to reflect the incident radiation avoids one of the essential inconveniences on the design that uses a metallic material: even though each metallic surface may be highly reflective, absorption always accompanies each reflection by a metallic surface. And for the trapped radiation, the heat shield may actually behave like a blackbody in that it absorbs practically all the incident radiation. However, a dielectric, depending on the spectral range, can be selected that absorbs essentially none of the incident radiant energy [*1*]. The reflection must be accomplished by backscattering in depth, because the surface of the probe is eroding rapidly during entry as the result of thermochemical ablation.

In the design of an ablative heat shield system, since the ultimate purpose of the ablation heat shield is to keep the internal temperature of the space vehicles at a safe level during entry, the transient heat conduction characteristics of the ablator may be critical in the selection of material and its thickness.

As suitable ablative materials, we may consider many candidates, such as polytetrafluoroethylene (PTFE) and silica (SiO_2). The behavior of these heat shield materials at high temperatures (over the melting point) is one of the most interesting problems. However, since the physical properties at high temperature are not clear, there are many unexplained problems. We may know those of PTFE compared with other heat shield materials.

There are many papers (e.g., Refs. 4–6) concerned with the ablation of PTFE and most of them have been developed on steady or quasi-steady ablation. However, it seems realistic to consider that ablation is an unsteady phenomenon, although it may attain to the steady state only in the case of a semi-infinite length body being exposed in a uniform high-enthalpy stream for a long time.

Clark [*7*] first proposed the two-layer model with emphasis on the phase change (i.e., second-order transition) of Teflon, especially on the development of the gel layer. In his investigation, the transient one-dimensional ablation of Teflon was considered.

Arai applied the two-layer model to the axisymmetric model of Teflon with particular emphasis on the change in body shape and the instantaneous internal temperature distribution [*8*]. He got results that are in good agreement with his experimental data.

Holzknecht took account of the influence of the order of decomposition reaction and of the thermal expansion of PTFE [*9*]. Computed temperature profiles showed good agreement with measured distributions.

To the best of the author's knowledge, however, there is no paper except Kindler's paper [*10*], in which the effect of optical transmittance of PTFE on the temperature field and the mass loss rate are taken into account. He took the simple relationship

[11] for the total radiation flow that penetrates into the body. However, it does not sufficiently explain the effect of the incident radiation, especially, the scattering coefficient. In the gel layer, we may neglect the scattering coefficient compared with the absorption coefficient. On the other hand, in the solid layer (crystalline layer) we may not neglect it.

It is the purpose of this investigation to propose numerical results of the transient thermal response of PTFE. With particular emphasis on the effect of the second-order transition of PTFE and the incident radiation on the overall behavior of the transient temperature distribution inside the heat shield material, the formulation is made by use of the two-layer thermal model. The heat conduction equation is coupled with the radiation transfer equation and is solved by use of the shooting method to satisfy some boundary conditions. For this purpose, a one-dimensional heat conduction equation with temperature-dependent properties and the Kubelka-Munk "two-flux" equations will be investigated.

2. Analysis

2.1. *Physical Model*

PTFE is a milk-white, waxy, and partially crystalline (up to 80%) material at temperatures below 327°C. At 19°C and 30°C changes of chain configuration occur, but the involved heats of transition are negligible. The polymer undergoes a

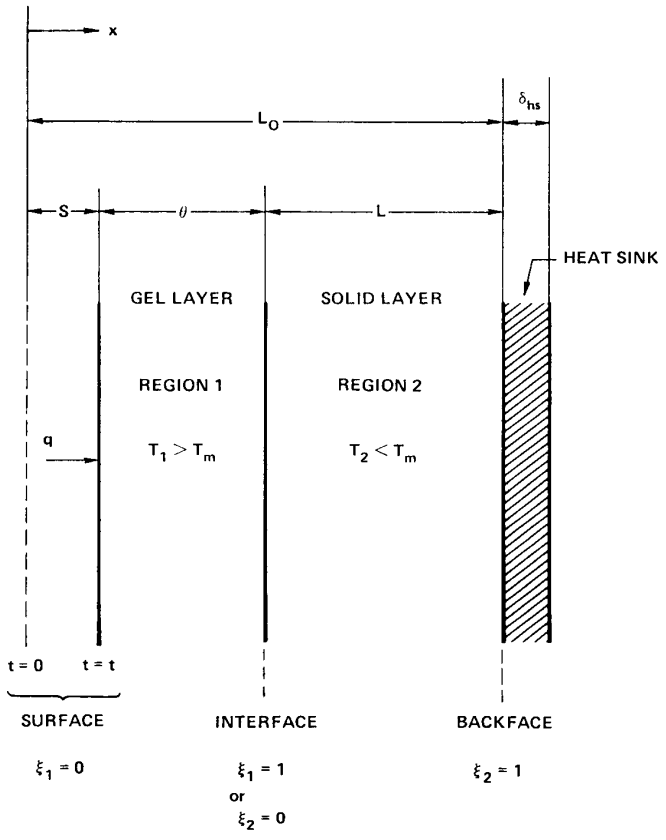

Fig. 1. Physical Model.

sharp, reversible transition at 327°C, changing from the white, translucent or opaque subtance to a transparent, amorphous material; the transition is accompanied by a heat of $h_m = 14$ cal/g. This major phase transition is usually called the "melting point." Although the melted PTFE should be considered as a liquid, its viscosity remains very high (e.g., 10^{11} poise in the temperature range from 330° to 390°C), so that the fluidity of the melted PTFE may be neglected. In this sense, the molten layer is called as a gel layer. As the temperature of PTFE is raised above 350°–400°C, pyrolysis occurs. The polymer decomposes into gaseous products without either charring or liquid layer formation. Though this decomposition is often called "sublimation," it is not a phase transition at a constant temperature, but a chemical reaction, namely the depolymerization of the polymer chains.

The two-layer thermal model is adopted in this paper. The physical model considered in this analysis is sketched in Fig. 1. A transient one-dimensional ablation model is chosen to represent the thermal response of a PTFE slab exposed to the external convective and radiative heat fluxes. The present analysis considers the heat transfer process only within the heat shield material under the conditions of given convective and radiative heating at the front surface. Thermal expansion is neglected.

2.2. *Governing Equations*

Consider a finite slab of PTFE with the exposed surface at $x=s$ receding at the ablation velocity $\dot{s}$ and the thickness θ of the gel layer at the growing rate $\dot{\theta}$. A heat sink is located at $x=L_0$. The phase transition plane divides the slab into two regions as shown: the gel layer (subscript 1) between s and $s+\theta$ where $T_1 > T_m$, and the solid layer (subscript 2) between $s+\theta$ and L_0 where $T_2 < T_m$.

Conservation of energy for a slab in which heat is conducted inwardly and radiation is being scattered, absorbed, and emitted in depth, may be expressed as

$$\rho_1 C_{p,1} \frac{\partial T_1}{\partial t} = \frac{\partial}{\partial x}\left(k_1 \frac{\partial T_1}{\partial x}\right) + Q_R + Q_P \tag{1}$$

$$\rho_2 C_{p,2} \frac{\partial T_2}{\partial t} = \frac{\partial}{\partial x}\left(k_2 \frac{\partial T_2}{\partial x}\right) + Q_R \tag{2}$$

where

$$Q_P = -A_p \rho_1 H_p(T) \exp\left(-\frac{E}{RT_1}\right)$$

$$Q_R = \pi \sum_{\nu=m}^{m'} K_\nu (I_{R,\nu} + I_{T,\nu} - 2n^2 I_{B,\nu}).$$

Q_P is the energy per unit volume bound by the depolymerization process not only at the surface but inside the body as well. This is the sink term in Eq. (1). On the other hand, Q_R means the radiative term and is the source term in Eqs. (1) and (2).

The inward and outward radiative fluxes are described by the Kubelka-Munk transfer equations [2] as

$$\frac{dI_{T,i,\nu}}{dx} = -(S_{i,\nu}+K_{i,\nu})I_{T,i,\nu}+S_{i,\nu}I_{R,i,\nu}+n_i^2K_{i,\nu}I_{B,i,\nu} \tag{3}$$

$$\frac{dI_{R,i,\nu}}{dx} = (S_{i,\nu}+K_{i,\nu})I_{R,i,\nu}-S_{i,\nu}I_{T,i,\nu}-n_i^2K_{i,\nu}I_{B,i,\nu} \tag{4}$$

where $i=1$ for the gel layer and 2 for the solid layer. K and S are the absorption coefficient and scattering coefficient, respectively.

2.3. *Boundary Conditions*

The surface temperature rises continuously and, consequently, the polymer chain is broken down and the ablative products go into the boundary layer. They react chemically with the oxygen in the boundary layer. The heat transfer to the surface is reduced as a result of the mass transport into the boundary layer and is increased due to the exothermic reaction. We consider that the incident flux is composed of radiation bands that either penetrate the material to be backscattered in depth or are absorbed at the surface [2]. That is, we define the incident flux

$$q_r = \sum_{\nu=m}^{m'} q_{r,\nu} + \sum_{\nu=n}^{n'} q_{r,\nu} \tag{5}$$

where the first sum is radiation that penetrates and is scattered and the last is surface absorbed radiation. Therefore, at the exposed surface, the flux conducted into the material is expressed as

$$-\left(k_1\frac{\partial T_1}{\partial x}\right)_s = \psi q_0\left(1+\frac{Ch_v}{\Delta H_w}\right)+q_{rad} \tag{6}$$

where q_0 stands for convective heating rate, ψ is the correction factor [5], [12] for incident convective fluxes by mass injection, and q_{rad} represents the total incident radiative flux expressed as

$$q_{rad} = \pi \sum_{\nu=n}^{n'} [(1-r_{s,e})I_{e,\nu}-\varepsilon I_B(T_w)]. \tag{7}$$

C represents the fraction of mass of oxygen in a flow and h_v the reaction heat per unit mass of oxygen. The correction factor for incident radiative fluxes is assumed to be 1.0.

The position of the surface is given by the ablation rate, which is here defined as the sum of the depolymerization products. When it is assumed that all the monomer leaves the body, the ablation rate is given by

$$\dot{m} \equiv \rho_0\frac{ds}{dt} = A_p\int_s^{s+\theta}\rho_1(\xi, t)\exp\left(-\frac{E}{RT_1}\right)d\xi \tag{8}$$

where ρ_0 is some reference density; the position of the surface is given by

$$s=\int_0^t \frac{ds}{dt}dt. \tag{9}$$

At the interface between the gel layer and the solid layer, the temperature must be continuous, that is,

$$T_1=T_m=T_2. \tag{10}$$

On the other hand, heat flux balance across the interface may be expressed as

$$-k_2\frac{\partial T_2}{\partial x}=-k_1\frac{\partial T_1}{\partial x}-\rho_m h_m\frac{d}{dt}(s+\theta) \tag{11}$$

where h_m is the latent heat for phase change from the solid to the gel and ρ_m is the mean density at the interface and is defined as $\rho_m=(\rho_1+\rho_2)/2$. Furthermore, in Eq. (11), it is assumed that the incident radiative flux is not absorbed at the interface.

For taking the heat sink into account at the backface, the boundary condition is expressed as

$$-k_2\frac{\partial T_2}{\partial x}+\pi\sum_{\nu=m}^{m'}(1-r_b)I_{T,2,\nu}=\rho_{hs}C_{p,hs}\delta_{hs}\frac{\partial T_2}{\partial t} \tag{12}$$

where ρ_{hs}, $C_{p,hs}$, and δ_{hs} represent the density, the specific heat, and the thickness of the heat sink, respectively.

The boundary conditions for this set of Kubelka-Munk transfer Eqs. (3) and (4) (see Fig. 2)
at the exposed surface:

$$I_{T,1}=(1-r_{s,e})I_e+r_{s,i}I_{R,1} \tag{13}$$

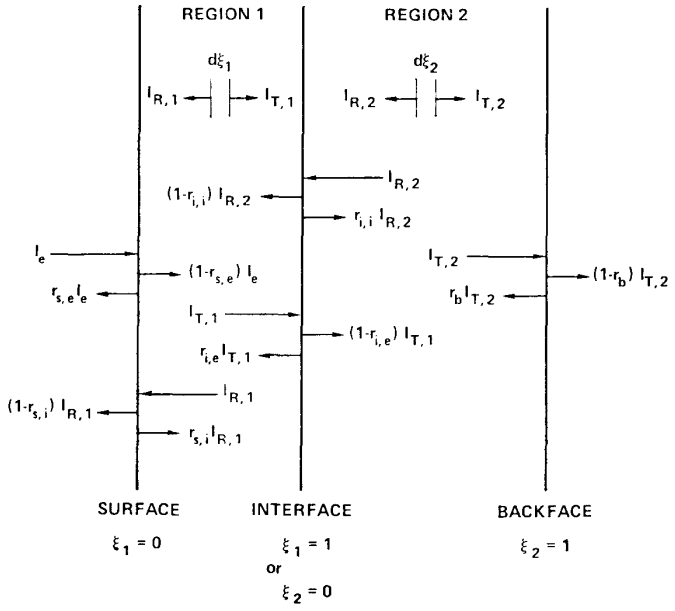

FIG. 2. Illustration of Radiative Transfer Model.

at the interface:

$$I_{R,1}=r_{i,e}I_{T,1}+(1-r_{i,i})I_{R,2} \tag{14}$$

$$I_{T,2}=(1-r_{i,e})I_{T,1}+r_{i,i}I_{R,2} \tag{15}$$

at the backface:

$$I_{R,2}=r_bI_{T,2} \tag{16}$$

2.4. *Initial Conditions*

The initial conditions that must be specified are the temperature distribution, the thickness of the gel layer, and the position of the surface. A prescribed initial temperature profile T_i is smaller than T_m (i.e., $T_i<T_m$), so that the gel layer does not exist initially. For this reason, the governing equation for a single-layer material must be first solved until the phase transition temperature T_m is reached at the exposed surface. After the surface temperature has risen to the phase transition temperature T_m, the governing equations for a two-layer material must be solved. For the most cases of interest, it may be reasonable to assume that the initial temperature distribution is uniform. Therefore, we define the initial conditions as

$$T(x, 0)=T_i \tag{17}$$

$$s=\theta=0. \tag{18}$$

It is assumed that the ablation does not occur till the surface temperature T_w reaches the phase transition temperature T_m. Once T_w is higher than T_m, the gel layer begins to develop. The initial growing rate of the gel layer is given by the surface energy balance at $T_w=T_m$. That is,

$$-\left(k_2\frac{\partial T_2}{\partial x}\right)_s=q_0+q_{rad}-\rho_2h_m\frac{d\theta}{dt}. \tag{19}$$

The thickness θ of the gel layer is given by integrating of the equation of $\dot{\theta}$ from $t=t_m$ to $t=t$. That is,

$$\theta=\int_{t_m}^{t}\frac{d\theta}{dt}dt. \tag{20}$$

2.5. *Variable Transformation*

For heat conduction problems involving surface recession, it is convenient to use a coordinate system that is fixed at the moving surface. Figure 1 is a schematic diagram in the transformed coordinate system. The spatial coordinate x is transformed into $\xi_i(i=1 \text{ or } 2)$ by the following expressions. Within the gel layer:

$$\xi_1=\frac{x-s(t)}{\theta(t)} \tag{21}$$

and within the solid layer:

$$\xi_2 = \frac{x-[s(t)+\theta(t)]}{L(t)} \tag{22}$$

where s is the change from its initial position due to surface recession, θ is the thickness of the gel layer, and L is the thickness of the solid layer. $\xi_1=0$ indicates the exposed surface, $\xi_1=1$ or $\xi_2=0$ the interface between the gel layer and the solid layer, and $\xi_2=1$ the backface.

The chain rule of differentiation appropriate to the transformation of the variable may be summarized as

$$\left.\begin{aligned} \frac{\partial}{\partial x} &= \frac{1}{\theta}\frac{\partial}{\partial \xi_1} \\ \frac{\partial}{\partial t} &= \frac{\partial}{\partial t} - \frac{1}{\theta}(\dot{s}+\xi_1\dot{\theta})\frac{\partial}{\partial \xi_1} \end{aligned}\right\} \text{region 1}$$

$$\left.\begin{aligned} \frac{\partial}{\partial x} &= \frac{1}{L}\frac{\partial}{\partial \xi_2} \\ \frac{\partial}{\partial t} &= \frac{\partial}{\partial t} - \frac{1-\xi_2}{L}(\dot{s}+\dot{\theta})\frac{\partial}{\partial \xi_2} \end{aligned}\right\} \text{region 2} \tag{23}$$

By use of Eq. (23), energy equations, Eqs. (1) and (2), can be reduced to, respectively:

$$\rho_1 C_{p,1}\frac{\partial T_1}{\partial t} = \frac{1}{\theta^2}\frac{\partial}{\partial \xi_1}\left(k_1\frac{\partial T_1}{\partial \xi_1}\right) + \frac{\rho_1 C_{p,1}}{\theta}(\dot{s}+\xi_1\dot{\theta})\frac{\partial T_1}{\partial \xi_1} + Q_R + Q_P \tag{24}$$

$$\rho_2 C_{p,2}\frac{\partial T_2}{\partial t} = \frac{1}{L^2}\frac{\partial}{\partial \xi_2}\left(k_2\frac{\partial T_2}{\partial \xi_2}\right) + \frac{\rho_2 C_{p,2}}{L}(1-\xi_2)(\dot{s}+\dot{\theta})\frac{\partial T_2}{\partial \xi_2} + Q_R. \tag{25}$$

Furthermore, the Kubelka-Munk transfer Eqs. (3) and (4) can be rewritten as, respectively:

$$\frac{1}{\theta}\frac{dI_{T,1,\nu}}{d\xi_1} = -(S_{1,\nu}+K_{1,\nu})I_{T,1,\nu} + S_{1,\nu}I_{R,1,\nu} + n_1^2 K_{1,\nu}I_{B,1,\nu} \tag{26}$$

$$\frac{1}{\theta}\frac{dI_{R,1,\nu}}{d\xi_1} = (S_{1,\nu}+K_{1,\nu})I_{R,1,\nu} - S_{1,\nu}I_{T,1,\nu} - n_1^2 K_{1,\nu}I_{B,1,\nu} \tag{27}$$

$$\frac{1}{L}\frac{dI_{T,2,\nu}}{d\xi_2} = -(S_{2,\nu}+K_{2,\nu})I_{T,2,\nu} + S_{2,\nu}I_{R,2,\nu} + n_2^2 K_{2,\nu}I_{B,2,\nu} \tag{28}$$

$$\frac{1}{L}\frac{dI_{R,2,\nu}}{d\xi_2} = (S_{2,\nu}+K_{2,\nu})I_{R,2,\nu} - S_{2,\nu}I_{T,2,\nu} - n_2^2 K_{2,\nu}I_{B,2,\nu}. \tag{29}$$

2.6. *Numerical Calculation*

The system of equations for the transient ablation consists of three differential equations in the crystalline phase, three differential equations in the amorphous phase, and the corresponding boundary conditions. These equations are nonlinear

because of moving boundaries, the temperature dependence of the thermophysical properties, and the chemical reaction. After transformation to constant boundaries, the system of equations is solved by an implicit finite difference method and the R-K-G method.

In the governing Eqs,. (24–29), the ablation rate $\dot{m}$ (or recession rate $\dot{s}$), $\dot{\theta}$ and $I_{T,1}$ (or $I_{R,1}$) at the exposed surface are three of the unknown variables. By assuming $\dot{\theta}$ and $I_{T,1}$ (or $I_{R,1}$) and taking $\dot{m}$ as a parameter, the next relation can be obtained by solving Eqs. (24–29) to satisfy the boundary conditions (6), (11), and (16) by use of the shooting method.

$$T_w = F(\dot{m}). \tag{30}$$

On the other hand, the surface temperature T_w and the ablation rate $\dot{m}$ are correlated by introducing another chemical relation:

$$T_w = G(\dot{m}). \tag{31}$$

Equation (8) is used for Eq. (31).

Thus, two relations are obtained that give the desired solutions for an ablation

Table 1. Properties of Teflon

Property	Value	Dimension	Reference
k_1	$(21.04-3.34\times10^{-2}T/K+1.39\times10^{-5}T^2/K^2)\times10^{-4}$	$cal\cdot cm^{-1}\cdot sec^{-1}\cdot K^{-1}$	9
k_2	$(1.2+1.467\times10^{-2}T/K)10^{-4}$	$cal\cdot cm^{-1}\cdot sec^{-1}\cdot K^{-1}$	9
$C_{p,1}$	$0.216+0.156\times10^{-3}T/K$	$cal\cdot g^{-1}\cdot K^{-1}$	9
$C_{p,2}$	$0.123+0.3733\times10^{-3}T/K$	$cal\cdot g^{-1}\cdot K^{-1}$	9
ρ_1	$2.07-7\times10^{-4}T/K$	$g\cdot cm^{-3}$	9
ρ_2	$2.119+7.92\times10^{-4}T/K-2.105\times10^{-6}T^2/K^2$	$g\cdot cm^{-3}$	9
K_1	0.22	cm^{-1}	13
K_2	0.056	cm^{-1}	13
S_1	$\leq10^{-6}$	cm^{-1}	13
S_2	18	cm^{-1}	13
$r_{s,e}$	0.053 (if $T_w>T_m$), 0.071 (if $T_w\leq T_m$)		13
$r_{s,i}$	0.39 (if $T_w>T_m$), 0.50 (if $T_w\leq T_m$)		13
$r_{i,e}$	0.023		13
$r_{i,i}$	0.17		13
r_b	0.80		13
n_1	1.25		13, 17
n_2	1.36		13, 17
ε	0.1		14
H_p	$424-6.67\times10^{-2}T/K$	$cal\cdot g^{-1}$	15
h_m	14	$cal\cdot g^{-1}$	16
h_v	5.66×10^3	$cal\cdot g^{-1}$	12
E	7.56×10^4	$cal\cdot mole^{-1}$	9
A_p	3.1×10^{19}	sec^{-1}	9

rate $\dot{m}$ and surface temperature T_w. The desired $\dot{m}$ and T_w can be found graphically or numerically from relations (30) and (31). Then the governing Eqs. (24–29) are again solved by using the above obtained $\dot{m}$ and T_w, and at last the temperature distribution, radiation intensity distributions, ablation rate $\dot{m}$, and the growing rate $\dot{\theta}$ of the gel layer are obtained.

The numerical computation was carried out by the following procedure. Since the prescribed initial temperature distribution is lower than the phase transition temperature T_m, the governing equations are first solved by using the single-layer thermal model up to the time the phase transition temperature is reached on the surface. With the temperature distribution at this time as an initial condition, the calculation is continued further by using the two-layer thermal model over the specified time period.

The thermal and optical properties of Teflon are shown in Table 1.

3. Discussion of Results

One of the main purposes of this investigation was to investigate the effect of radiative heating on the thermal field in the heat shield; the heat field is represented by the two-layer thermal model. In the sample calculations from Figs. 3–9, $L_0 = 1.0$ cm,

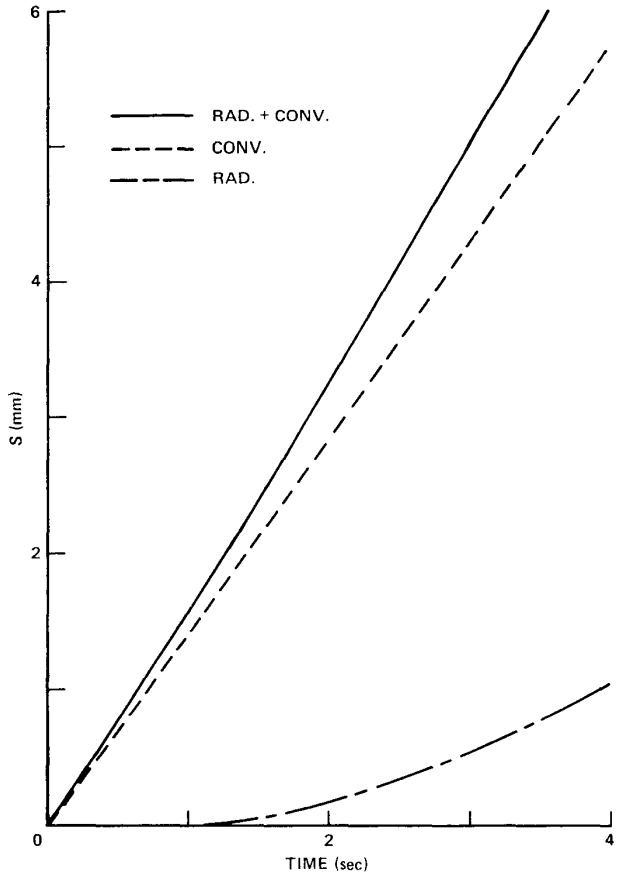

Fig. 3. History of Recession Depth. $H_0 = 1000$ cal/g, $q_0 = 100$ cal/sec/cm^2, $q_r = 250$ cal/sec/cm^2.

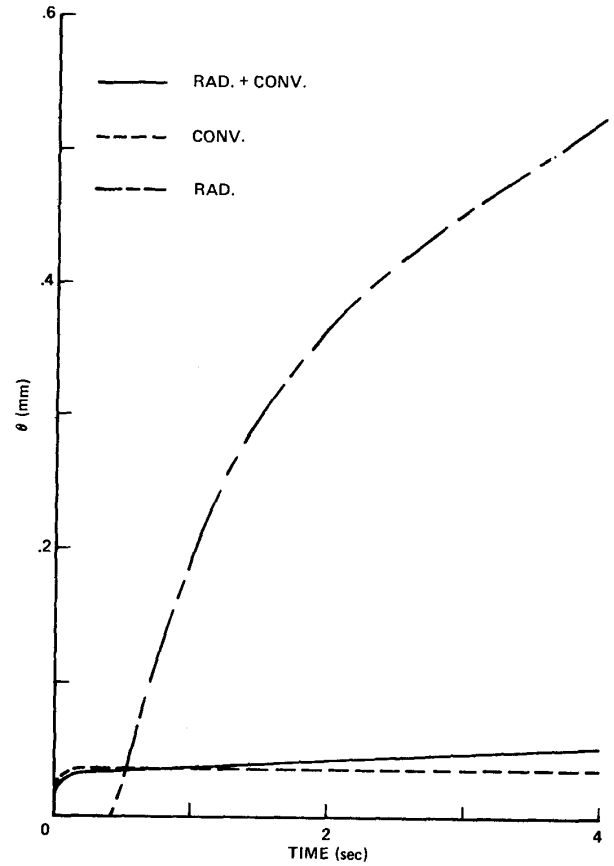

FIG. 4. History of the Thickness of Gel Layer. $H_0=1000$ cal/g, $q_0=100$ cal/sec/cm^2, $q_r=250$ cal/sec/cm^2.

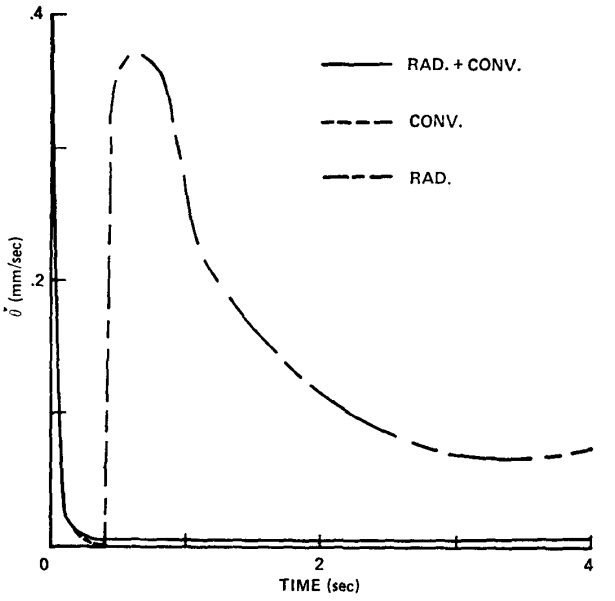

FIG. 5. Growing Rate the of Gel Layer. $H_0=1000$ cal/g, $q_0=100$ cal/sec/cm^2, $q_r=250$ cal/sec/cm^2.

$H_0 = 1000$ cal/g, $q_0 = 100$ cal/sec/cm^2, and $q_r = 250$ cal/sec/cm^2. (Of the incident radiation, we estimate that 96.5% penetrates and 3.5% is absorbed at the surface.) It is assumed that the backface is insulated.

Figure 3 shows the recession depth history. There is a great difference between the radiative heating only and other cases. This result is caused by the fact that a greater part of an incident radiative heating comes through the surface and penetrates into the material. The heat which is absorbed at the surface is very small. Therefore, the surface temperature increases very slowly compared with other cases and is lower than in other cases; consequently, the recession and the recession velocity are much smaller than other cases.

Figures 4 and 5 show the history of the thickness of the gel layer and the growing rate, respectively. In the case of radiative heating only, the gel is much thicker than in other cases. This may be explained as follows. The internal temperature increases mainly due to the absorption of the incident radiation, while the recession and the recession velocity in the case of radiative heating only are much smaller than in other cases. Therefore, the thickness keeps on increasing. In the case of the combined radiative and convective heating, the recession depth is large, so the gel is very thin and the growing rate is small. However, because of the incident radiation,

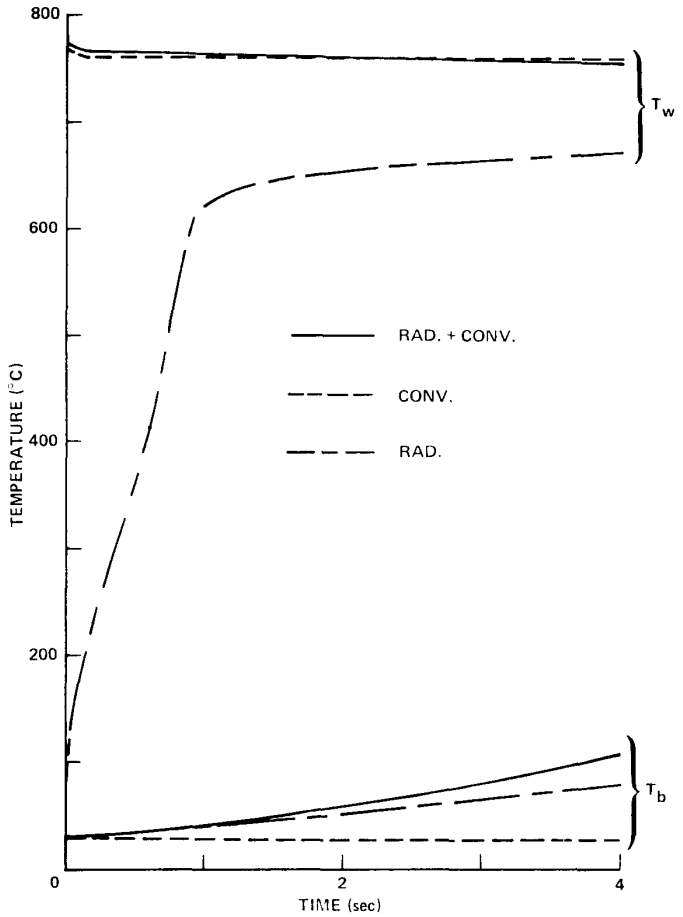

FIG. 6. Surface and Backface Temperature History. $H_0 = 1000$ cal/g, $q_0 = 100$ cal/sec/cm^2, $q_r = 250$ cal/sec/cm^2.

the thickness does not become constant. On the other hand, in the case of the convective heating only, it becomes almost constant at an early time.

Figure 6 shows the history of the surface and backface temperatures for every case. In the case of the combined heating and the convection only, the surface temperature increases abruptly and becomes almost constant very soon. On the other hand, in the case of the radiative heating only, it increases much more slowly than in other cases. This may be caused by the fact that only a small part of the radiative heating is absorbed at the surface and that a greater part of it penetrates into the material. In the case of convective heating only, the backface temperature does not increase; in other cases it continues to increase. It seems that this phenomenon is caused by the incident radiation. The backface temperature in the case of the radiative heating only is lower than in the case of the combined heating. This is due to the difference of the recession velocity. The thickness of the material in the former case is much greater than in the latter case. Therefore, the radiation is absorbed

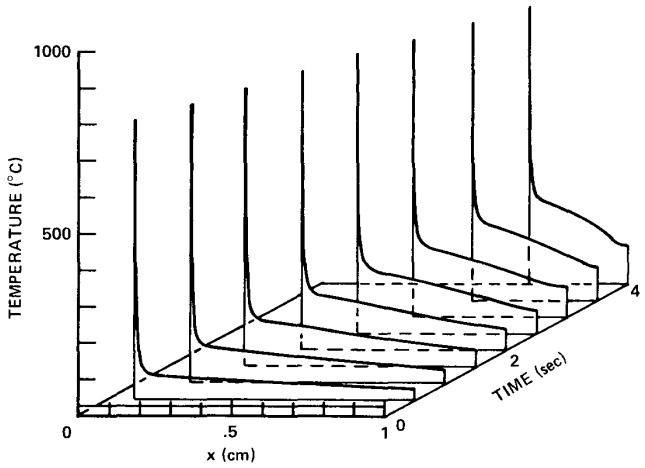

FIG. 7. Temperature Distribution as a Function of Time and Position with Combined Radiative and Convective Heating. $H_0=1000$ cal/g, $q_0=100$ cal/sec/cm^2, $q_r=250$ cal/sec/cm^2.

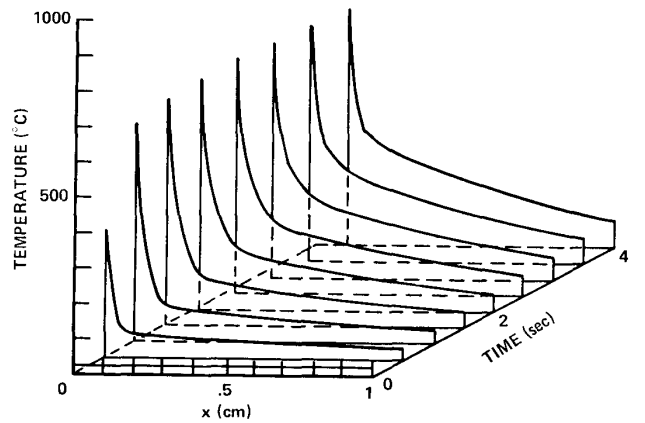

FIG. 8. Temperature Distribution as a Function of Time and Position with Radiative Heating only. $H_0=1000$ cal/g, $q_r=250$ cal/sec/cm^2.

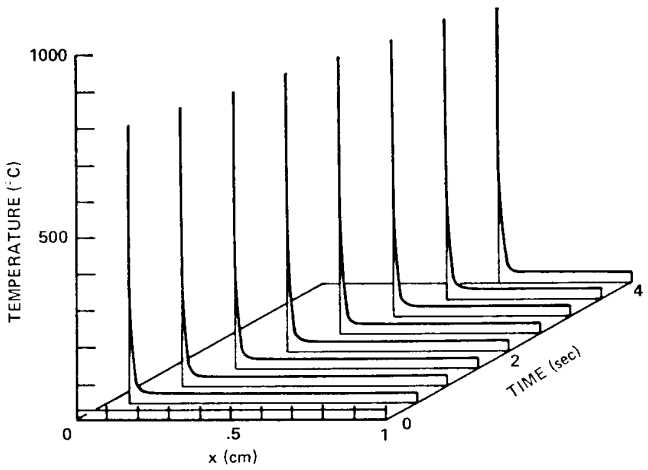

FIG. 9. Temperature Distribution as a Function of Time and Position with Convective Heating only. $H_0=1000$ cal/g, $q_0=100$ cal/sec/cm^2.

and scattered on the way and less of it reaches the backface. In the case of convective heating only, the backface temperature does not rise because of the low thermal diffusivity of Teflon.

Figures 7–9 show the instantaneous temperature distribution. As previously mentioned, a greater part of the rise in the internal temperature (except in the vicinity of the surface) seems to be caused by the absorption and the scattering of the incident radiation. When the thermal thickness is defined as

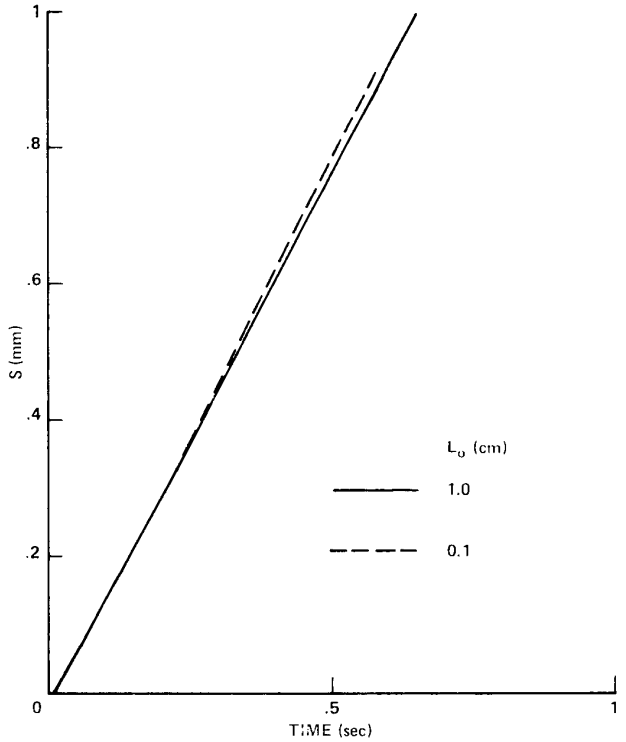

FIG. 10. History of Recession Depth. $H_0=1000$ cal/g, $q_0=100$ cal/sec/cm^2, $q_r=250$ cal/sec/cm^2.

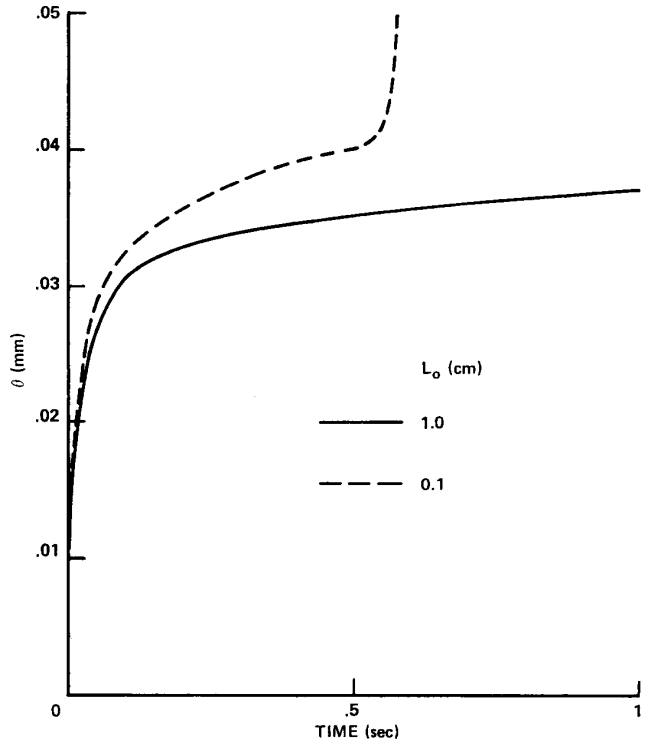

FIG. 11. History of the Thickness of Gel Layer. $H_0=1000$ cal/g, $q_0=100$ cal/sec/cm^2, $q_r=250$ cal/sec/cm^2.

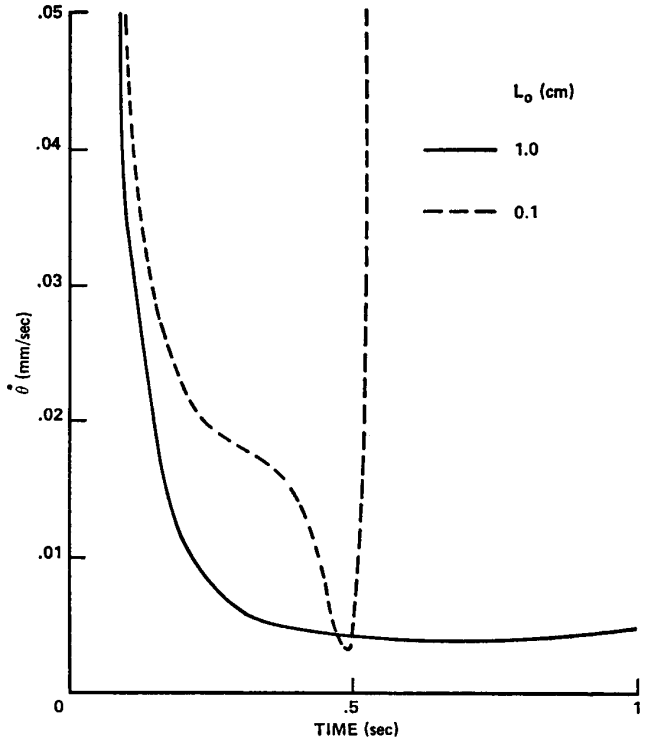

FIG. 12. Growing Rate of the Gel Layer. $H_0=1000$ cal/g, $q_0=100$ cal/sec/cm^2, $q_r=250$ cal/sec/cm^2.

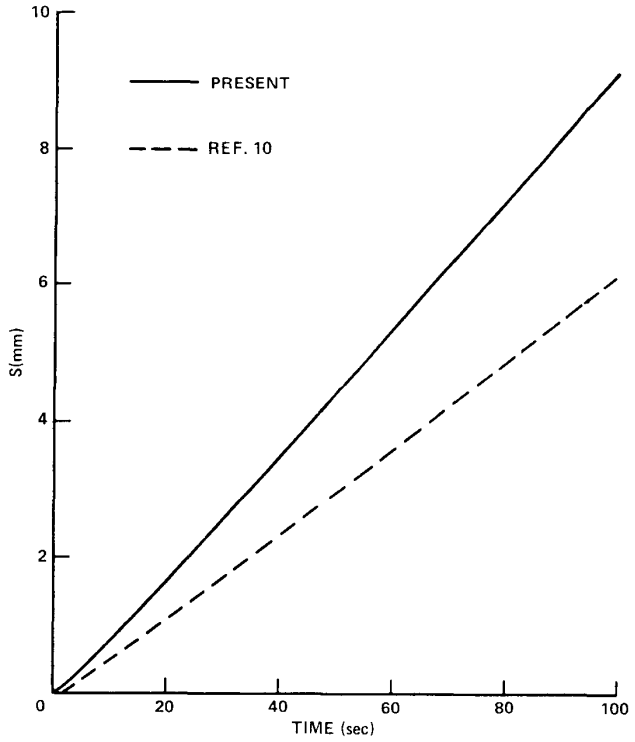

FIG 13. History of Recession Depth. $H_0=2127$ cal/g. $q_0=15.24$ cal/sec/cm^2, $q_r=1.69$ cal/sec/cm^2.

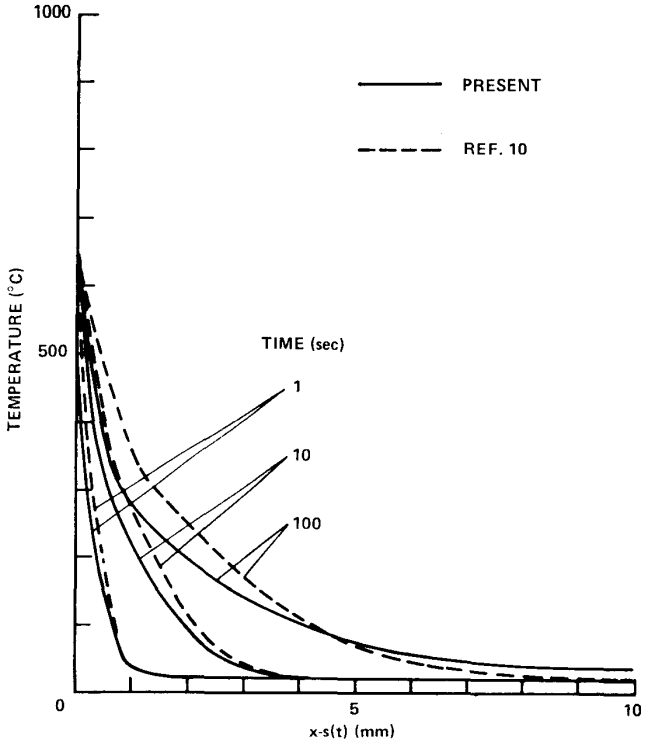

FIG. 14. Temperature Distribution in an Ablating Body. $H_0=2127$ cal/g, $q_0=15.24$ cal/sec/cm^2, $q_r=1.69$ cal/sec/cm^2.

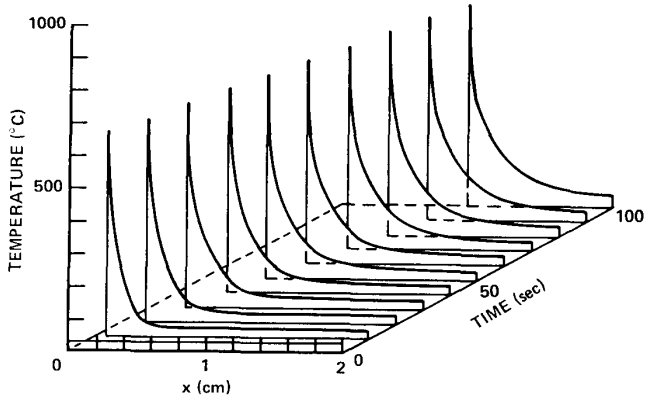

FIG. 15. Temperature Distribution as a Function of Time and Position $H_0=2127$ cal/g, $q_0=15.24$ cal/sec/cm^2, $q_r=1.69$ cal/sec/cm^2.

$$\delta=\frac{1}{T_w}\int_s^{L_0} T dx, \tag{32}$$

in the case of the convective heating only, it is much smaller than in other cases. The surface temperature is influenced by the convective heating. On the other hand, the rise in the internal temperature is influenced by the radiative heating.

The effect of the initial thickness of the heat shield is shown in Figs. 10–12. As shown in Fig. 10, both of the recession depth histories are almost the same. On the other hand, as shown in Figs. 11 and 12, histories of the thickness of the gel layer and of its growing rate show many differences. This may be caused by the difference in heat capacity. The thinner the heat shield, the sooner the internal temperature rises, and consequently, the gel layer is thicker. The sudden increasing of θ or $\dot{\theta}$ is caused by the fact that the thickness of the heat shield was reduced because of surface erosion.

The comparison with another theory [*10*] is shown in Figs. 13 and 14. Many differences of the recession depth history seem to be mainly due to differences in the physical properties. As shown in Fig. 14, however, the difference in the temperature distribution seems to be due not only to the differences in physical properties, but also to the difference in the estimation of incident radiation. In Ref. 10, the effect of the incident radiation is taken into account in the gel layer, but not in the solid phase. Therefore, the temperature at the backface in Ref. 10 does not rise as the present analysis. Figure 15 shows the instantaneous temperature distribution.

4. CONCLUSION

Investigation of the high temperature behavior of Teflon was taken as a basis for an analytical model of the transient ablation of Teflon under the condition in which the intense radiation is coupled with convective heating. The resulting system of differential equations was numerically solved.

The incident radiation causes significant changes in the growth process of the gel

layer and in the instantaneous temperature distribution. The surface temperature does not seem to be influenced by the radiation. However, the internal temperature seems to be significantly affected by it. In the case of convective heating only, the internal temperature is unaffected except near the surface. In other cases it rises throughout the material, such that (except in the vicinity of the surface) the difference becomes large. In the case of convective heating only, steady-state ablation seems to be reached at a very early time, while it does not seem to be reached when incident radiation is accounted for. The results of the present calculations confirm that the optical transmittance of both the amorphous zone (gel layer) and the crystalline zone cannot be neglected in considering the transient ablation under the condition of the radiative heating.

Acknowledgment

The author would like to express his gratitude to Drs. P. R. Nachtsheim and J. T. Howe of NASA Ames Research Center for their initiation of this work and for their very useful comments.

Department of Aerodynamics
Institute of Space and Aeronautical Science
University of Tokyo
January 11, 1979

References

[1] Nachtsheim, P. R., Peterson, D. L., and Howe, J. T., "Reflecting and Ablating Heat Shields for Radiative Environments," AAS Paper 71-147; also *Advances in the Astronautical Sciences*, Vol. 29 II, 1971, pp. 253-264.

[2] Howe, J. T., Green, M. J., and Weston, K. G., "Thermal Shielding by Subliming Volume Reflectors in Convective and Intense Radiative Environments," *AIAA Journal*, Vol. 11, No. 7, 1973, pp. 989-994.

[3] Howe, J. T. and McCulley, L. D., "Volume-Reflecting Heat Shield for Entry Into the Giant Planet Atmospheres," AIAA Paper 74-669, 1974.

[4] Adams, M. L., "Recent Advances in Ablation," *ARS Journal*, Vol. 29, 1959, pp. 625-632.

[5] Marvin, J. G. and Pope, R. B., "Laminar Convective Heating and Ablation in the Mars Atmosphere," *AIAA Journal*, Vol. 5, No. 2, 1965, pp. 240-248.

[6] Newman, R. L., "A Kinetic Treatment of Ablation," *Journal of Spacecraft*, Vol. 2, No. 3, 1965, pp. 449-452.

[7] Clark, B. L., "A Parametric Study of the Transient Ablation of Teflon," *Journal of Heat Transfer*, Vol. 94 C, No. 4, 1972, pp. 347-354.

[8] Arai, N., "A Study of Transient Thermal Response of Ablation Materials," ISAS Rept. 544, Institute of Space and Aeronautical Science, University of Tokyo, Sept. 1976.

[9] Holzknecht, B., "An Analytical Model of The Transient Ablation of Polytetrafluoroethylene Layers," *International Journal of Heat and Mass Transfer*, Vol. 20, No. 6, 1977, pp. 661-668.

[10] Kindler, K., "Experimentelle Untersuchung des Ablationsverhaltens von einfachen Körpern unterschiedlicher Nasenform und Materialzusammensetzung," Deutsche Forschungs- und Versuchsanstalt für Luft- und Raumfahrt, Institut für Angewandte Gasdynamik, Köln, DLR-FB 76-08, Jan. 1976.

[11] Munson, T. R. and Spindler, R. J., "Transient Thermal Behaviour of Decomposing Materials. Part I: General Theory and Application to Convective Heat," IAS Paper 62–30, 1962.

[12] Pope, R. B., "Simplified Computer Model for Predicting the Ablation of Teflon," *Journal of Spacecraft and Rockets*, Vol. 12, No. 2, 1975, pp. 83–88.

[13] Congdon, W. M., "Reflecting Heat-Shield Entry Analysis Computer Program for Planetary Probes," AIAA Paper 73–714, 1973.

[14] Nicolet, W. E., Howe, J. T., and Mezines, S. A., "Outer Planet Probe Entry Thermal Protection: Part II: Heat-Shielding Requirements," AIAA Paper 74–701, 1974.

[15] Kemp, N. H., "Surface Recession Rate of an Ablating Polymer," *AIAA Journal*, Vol. 6, No. 9, 1968, pp. 1790–1791.

[16] Wentink, T., Jr., "High Temperature Behaviour of Teflon," Avco Research Lab. Rept. 55, 1959.

[17] MaCane, D. I., "Tetrafluoroethylene Polymers, Polytetrafluoroethylene," Encyclopedia of Polymer Science and Technology, New York: John Wiley & Sons Inc., 1970, Vol. 13, pp. 623–654.